Available online at www.sciencedirect.com
SCIENCE DIRECT
Carbohydrate Polymers 59 (2005) 339–350
Carbohydrate Polymers
www.elsevier.com/locate/carbpol

Modelling the rheological behaviour of galactomannan aqueous solutions

W. Sittikijyothin, D. Torres, M.P. Gonçalves*

REQUIMTE, Departamento de Engenharia Química, Faculdade de Engenharia da Universidade do Porto, Rua Dr. Roberto Frias, s/n, 4200-465 Porto, Portugal

Received 12 July 2004; revised 17 September 2004; accepted 5 October 2004
Available online 29 December 2004

Abstract

The rheological behaviour of aqueous galactomannan—tara gum (TG) and locust bean gum (LBG)—solutions was studied at 25 °C, using steady-shear and dynamic oscillatory measurements performed with a controlled stress rheometer AR2000 (TA Instruments) fitted with cone-and-plate geometry. The intrinsic viscosity of LBG, $[\eta]=11.03$ dl/g, was lower than those for crude ($[\eta]=14.96$ dl/g) and purified ($[\eta]=16.46$ dl/g) TG. The plot of the specific viscosity at zero shear rate vs the coil overlap parameter, $C[\eta]$, revealed a similar behaviour for both galactomannans: a master curve could be obtained with a critical concentration C^{**} (the upper limit of the semi-dilute regime) $\sim 7.76/[\eta]$ and a slope of 4.7 in the concentrated regime. Experimental data in steady shear (flow curves) have been correlated with the Cross and Carreau models. Both models described the apparent viscosity shear rate data well. In general, the Cross model provided a slightly better fit. In the concentrated regime, it was possible to obtain a master flow curve for both galactomannans after performing a concentration-dependent shift using the 1 wt% LBG solution as the reference. Master curves were also obtained, in oscillatory shear, for $G'(\omega)$ and $G''(\omega)$ plots, by shifting along the two axes. The vertical and horizontal shift factors were the same for both $G'(\omega)$ and $G''(\omega)$ curves. Two mechanical models were used for fitting the experimental data (mechanical spectra): the generalized Maxwell model with four elements and the Friedrich–Braun model. Both models correlate the experimental data very well. The correlation between dynamic and steady-shear properties (Cox–Merz rule) was satisfactory for the two galactomannans.

Keywords: Rheology; Viscoelasticity; Galactomannans; Tara gum; Locust bean gum

1. Introduction

The human race has a long history of exploiting plant polysaccharides—for example starch, in foods, and cellulose for clothing materials. In more recent years, gums have been employed in a wide variety of industrial and food applications. The former include oil well fracturing and drilling, paper manufacture (as strengthening agents), rheology (flow) control in latex paints and uses as thickeners and gels in blasting agents and as thickeners in various cosmetics. The food industry makes use of gums most often as additives to control functional properties of (food) products.

Many gums are extracted from plants. Tara gum (TG), locust bean gum (LBG) and guar gum (GG) are galactomannans extracted by grinding the endosperm portions of the seeds of the legume plants *Caesalpinia spinosa*, *Ceretonia siliqua* L., and *Cyamopsis tetragonolobus*, respectively. Galactomannans are neutral polysaccharides composed of linear main chains of β-1→4 linked mannose units with α-1→6 linked side chains of a single galactose unit. They differ in the ratio of mannose to galactose units, M/G. The more substituted of the commercial galactomannans is guar gum (M/G ∼ 2:1); in tara gum, the M/G is ∼3:1 while in locust bean gum is ∼4:1 (Alais & Linden, 1991; Batlle & Tous, 1997; Mc Cleary & Neukom, 1982; Ruiz-Ángel, Simó-Alfonso, Mongay-Fernández, & Ramis-Ramos, 2002) (Fig. 1). The great advantage of galactomannans is their ability, at relatively low concentrations, to form very viscous solutions that are only slightly affected by pH, added ions, and heat processing.

The structural characteristics of galactomannans, especially guar gum and locust bean gum, have been extensively studied by several researchers (for example, Courtois & Le Dizet, 1966; Mc Cleary, Clark, Dea, & Rees, 1985). Their functional

* Corresponding author. Tel.: +351 22 508 1684; fax: +351 22 508 1449.
E-mail address: pilarg@fe.up.pt (M.P. Gonçalves).

0144-8617/$ - see front matter © 2004 Elsevier Ltd. All rights reserved.
doi:10.1016/j.carbpol.2004.10.005

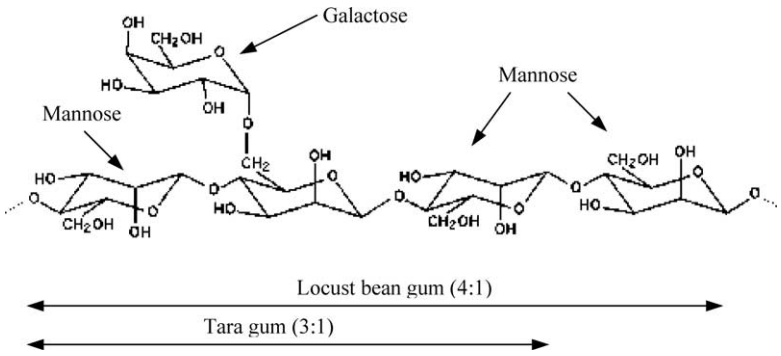

Fig. 1. Schematic illustration of the structures of locust bean gum and tara gum.

properties are related to both the structural features and the molecular masses. For similar M/G ratios, differences in the interaction properties have been detected between galactomannans of different sources, which were attributed to differences in their fine structures (Dea, Clark, & Mc Cleary, 1986). For similar molecular masses, locust bean gum and guar gum give solutions of similar viscosity but with quite different synergistic interactions; the M/G ratio seems to be the main factor for these different behaviour (Dea, Morris, Rees, Welsh, Barnes, & Price, 1977; Fernandes, Gonçalves, & Doublier, 1991). It has been shown that guar gum and locust bean gum show similar relationships between the specific viscosity at 'zero' shear rate and the product of the concentration and intrinsic viscosity, $C[\eta]$ (the coil overlap parameter). The behaviour is of the same pattern as that shown for synthetic polymers and several random coil polysaccharides. However, for the two galactomannans, higher viscosities were observed for concentrations above that at which entanglements form. This has been attributed to the presence of more specific interactions between the macromolecules ('hyperentanglements'), in addition to the non-specific physical entanglements, by Morris, Cutler, Ross-Murphy, Rees, and Price (1981). These authors also observed the same shear thinning profile for different polysaccharides irrespective of chemical type, concentration or molecular weight. This has been interpreted as reflecting the existence of non-specific physical entanglements in the polysaccharide solutions. Flow master curves could be obtained by shifting along the two axes the flow curves obtained at different concentrations of the polysaccharides solutions. By using a similar reduced variables procedure, other authors obtained master flow curves for sodium alginate, lambda-carrageenan (Gonçalves, 1984) and cellulose derivatives (Castelain, Doublier, & Lefebvre, 1987). Many equations have been proposed to describe the shear thinning behaviour of solutions of coil-type macromolecules, like galactomannans; those of Carreau (1972) and Cross (1965) were successfully used by Alves, Garnier, Lefebvre, and Gonçalves (2001) and da Silva, Gonçalves, and Rao (1992) to study the flow behaviour of locust bean gum alone and in mixtures with pectins or gelatin; more recently, Oblonsek, Sostar-Turk, and Lapasin (2003) used the Cross model to describe the flow properties of concentrated guar gum solutions. Dynamic measurements have been extensively used to study viscoelasticity of polysaccharide solutions. For several galactomannans and other random-coil polysaccharides, at relatively high concentrations, a liquid-like behaviour was observed at low frequencies (G'' (dissipative modulus) $> G'$ (conservative modulus)); at higher frequencies, the system behaved like a solid, with $G' > G''$, and the 'cross-over frequency' (where $G' = G''$) typically moved to lower frequency values when the concentration increased (Andrade, Azero, Luciano, & Gonçalves, 1999; da Silva, Gonçalves, & Rao, 1993; Oblonsek et al., 2003; Robinson, Ross-Murphy, & Morris, 1982). As has been done with flow curves, master curves can be obtained for G' and G'' by superimposing curves obtained at different concentrations. The approaches to model the viscoelastic behaviour fall into two main categories: the molecular and the phenomenological approaches. The former is based on the definition of rheological properties starting from molecular or microscopic parameters, which identify the components of the system. The latter deals with the development and definition of the model according to the principles of continuum mechanics; it is based upon achieving the maximum agreement between predicted and experimental data. Using this last approach, the dynamic response of viscoelastic materials can be described using a generalized Maxwell model or the Friedrich–Braun model (1992), which belongs to the class of the fractional derivative models. These two models were used to describe the frequency dependence of G' and G'', in the linear viscoelastic regime, for different polysaccharides such as guar gum (Oblonsek et al., 2003), welan, gellan and carboxymethylcellulose (Manca, Lapasin, Partal, & Gallegos, 2001; Zupancic & Zumer, 2001).

In the present work, the rheological behaviour, in steady and dynamic shear conditions, of tara gum, a less studied galactomannan, was investigated and compared to that of locust bean gum in order to see if a generalized behaviour could be established for these two galactomannans. The flow and the viscoelastic properties of tara and locust bean gum solutions were studied for relatively high concentrations (semi-dilute and concentrated regimes), at 25 °C. For each polysaccharide, analysis of flow data was done using the Cross and Carreau models. Viscoelastic data were fitted with the Maxwell and Friedrich–Braun models.

The applicability of the coil overlap parameter as a generalized parameter to characterize flow behaviour was tested. Time-concentration superposition principle was applied to data of both galactomannans.

2. Materials and methods

2.1. Materials

Commercial samples of tara gum (TG, REF 1760) and locust bean gum (LBG, H01091-990), were kindly supplied by Carob SA (Spain) and Degussa Texturant Systems (France), respectively. Tara gum was purified by precipitation with isopropanol, as previously described (da Silva & Gonçalves, 1990).

2.2. Methods

2.2.1. Physicochemical analysis

Moisture and ash contents were determined according to Food Chemicals Codex (FCC III, 1981). The mannose/galactose ratios (M/G) of both galactomannans were determined by the method described by Coimbra, Delgadillo, Waldron, and Selvendran (1996).

Viscosity of dilute solutions was measured at 25.0 ± 0.1 °C with a capillary Cannon Fenske viscometer (ASTM-D2515, ISO 3105, Series 100), using exactly 10 ml of solution sample. Solutions had relative viscosities from about 1.2 to 2.0 to assure good accuracy and linearity of extrapolation to zero concentration. The limiting viscosity number ('intrinsic viscosity'), $[\eta]$, was obtained by double extrapolation to zero concentration of Huggins' and Kraemer equations, respectively

$$\frac{\eta_{sp}}{C} = [\eta] + k'[\eta]^2 C \quad (1)$$

$$\frac{(\ln \eta_{rel})}{C} = [\eta] + k''[\eta]^2 C \quad (2)$$

where η_{rel} and η_{sp} are the (dimensionless) relative and specific viscosities, k' and k'' are the Huggins' and Kramer's coefficients, respectively, and C is the solution concentration.

Viscosity average molecular masses, $\bar{M}_v$, were calculated using the Mark–Houwink relationship given by Doublier and Launay (1981) for guar gum as modified by Gaisford, Harding, Mitchell, and Bradley (1986) to take into account the different mannose:galactose ratios (M/G) of the galactomannans

$$[\eta] = 11.55 \times 10^{-6}[(1-\alpha)\bar{M}_v]^{0.98} \quad (3)$$

where $\alpha = 1/[(M/G)+1]$ and $[\eta]$ is expressed in dl/g.

2.2.2. Preparation of solutions

The required amount of the powdered gum was gradually added to the appropriate amount of distilled water in the presence of sodium azide (5 ppm) in order to prevent bacterial degradation. The dispersion was vigorously stirred for 1 h, at room temperature, followed by heating the dispersion at 80 °C in a water bath for 30 min, under continuous stirring. The non-dissolved material was removed by centrifugation at 30,000*g* for 1 h, at 25 °C and the concentration of the solutions was determined from their dry matter contents.

2.2.3. Rheological measurements

All rheological measurements were performed at 25 °C using a controlled stress rheometer AR2000 (TA Instruments) fitted with a cone-and-plate geometry (2° cone angle, 40 mm diameter, 54 μm gap). Aqueous solutions of locust bean gum (LBG, 0.4–1 wt%), crude tara gum (cTG, 0.25–1.29 wt%,) and purified tara gum (pTG, 0.25–1.19 wt%) were used. Dynamic measurements and frequency sweeps were performed in the 0.1–100 rad s^{-1} range, with strain amplitude of 5%, in order to assure working conditions inside the linear viscoelastic region. Steady shear data were recorded first in increasing order and then in decreasing order of applied torque. The torque was imposed using a logarithmic ramp, in order to decrease the initial acceleration and the effects due to instrument inertia. In all experiments, the samples were covered with a thin layer of paraffin oil to prevent evaporation.

3. Results and discussion

3.1. Characterisation of TG and LBG samples

In Table 1, the main characteristics of the galactomannan samples are presented. With the purification process used for TG, the ash content was drastically reduced and the M/G ratio increased. This increase of M/G may be due to the elimination of small and highly substituted molecules, with low M/G, which are more soluble and, consequently, are not precipitated by isopropanol during the purification step. The obtained values (≅3) are in good agreement with those reported by Morris (1990) (M/G≅2.7–3.0) and Fernandes et al. (1991) (M/G = 3.1). The M/G ratio for LBG is close to values in the literature: ≅3.5 (Morris, 1990), 3.85 (Alves, Antonov, & Gonçalves, 1999) and 3.30 (Andrade et al., 1999).

Table 1
Chemical composition of tara gum (TG) and locust bean gum (LBG) samples

	TG		LBG
	Crude	Purified	
Moisture	11.22 ± 0.01	7.81 ± 0.44	6.41 ± 0.07
Ash	0.77 ± 0.02	0.07 ± 0.02	0.80 ± 0.03
M/G	2.95 ± 0.04	3.03 ± 0.07	3.63 ± 0.09

All values (%) are mean ± standard deviation of three determinations.

Table 2
Physical–chemical parameters of tara gum (TG) and locust bean gum (LBG) samples

	TG		LBG
	Crude	Purified	
Intrinsic viscosity, at 25 °C (dl/g)	14.96	16.46	11.03
Huggins' coefficient, k'	0.79	0.57	0.84
Viscosity average molecular mass, $\bar{M}_v \times 10^{-6}$	2.31	2.53	1.61

Intrinsic viscosities and $\bar{M}_v$, for crude and purified TG, are higher than for LBG, as shown in Table 2. It can be seen that, for purified TG, a higher value of the intrinsic viscosity was obtained; a decrease in the magnitude of Huggins' coefficient, k', was also observed. Values for k' depend on solute–solvent interactions and on the state of aggregation of macromolecules; in theory, values are independent of molecular masses. In a good solven and for flexible macromolecules, $k' \sim 0.3$; but, it can be higher than 1 in case of aggregation. Values of 0.57–0.84, in Table 2, may reflect some intermolecular aggregation in our samples. In general, our results for k' and $[\eta]$ are quite consistent with others previously reported (Alves et al., 1999; da Silva & Gonçalves, 1990; da Silva & Rao, 1992).

3.2. Steady-shear properties

Typical flow curves, at 25 °C, for TG and LBG solutions, at different concentrations, are shown in Fig. 2. In all cases, the behaviour was shear-thinning with a Newtonian region in the low shear rate range. However, for similar concentrations, (i) LBG solutions were less viscous than TG solutions, which reflects the differences in intrinsic viscosity of the samples, and (ii) the shear-thinning behaviour appeared at a higher shear rate for LBG. The shear-thinning behaviour may be regarded as arising from modifications in macromolecular organisation in the solution as the shear rate changes. At low shear rates,

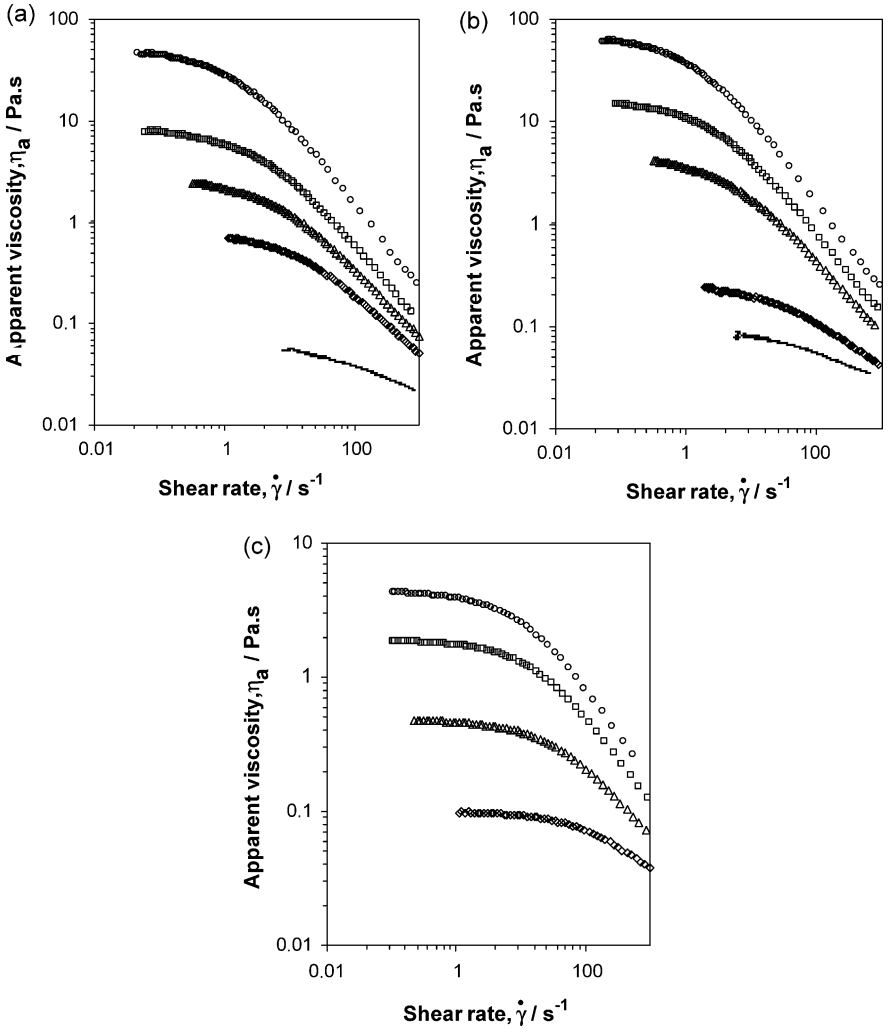

Fig. 2. Flow curves of galactomannan solutions at different concentrations (wt%), at 25 °C; (a) crude tara gum, 0.25% (–), 0.50% (◇), 0.64% (△), 0.78% (□) and 1.29% (○); (b) purified tara gum, 0.25% (–), 0.40% (◇), 0.64% (△), 0.88% (□) and 1.19% (○); (c) locust bean gum, 0.4% (◇), 0.6% (△), 0.8% (□) and 1.0% (○).

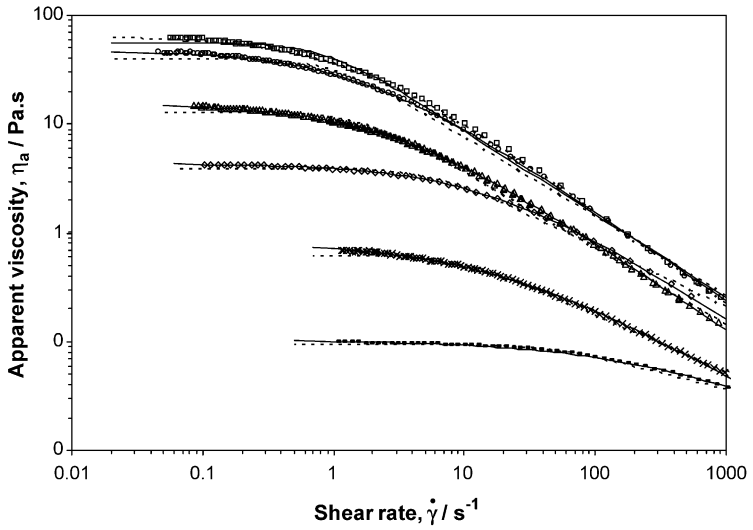

Fig. 3. Flow curves for crude tara gum, purified tara gum and locust bean gum samples at 25 °C. Symbols: 0.4% LBG (–), 0.5% cTG (×), 1.0% LBG (◇), 0.88% pTG (△), 1.29% cTG (○) and 1.19% pTG (□); Full line represents predictions of the Cross model and dotted lines those of the Carreau model.

the disruption of entanglements by the imposed shear is balanced by the formation of new ones, so that no net change in entanglements occurs; it is the Newtonian plateau region, where the viscosity has a constant value, the zero-shear rate apparent viscosity, η_0. For higher shear rates, disruption predominates over formation of new entanglements, molecules align in the direction of flow and the apparent viscosity decreases with increasing shear rate. As a consequence, the shear rate corresponding to the transition from Newtonian to shear-thinning behaviour moves to lower values as the concentration increases.

Carreau (1972, Eq. (5)) and Cross (1965, Eq. (4)) flow models have been used to describe the shear-thinning behaviour of the TG and LBG solutions

$$\eta_a = \eta_\infty + \frac{(\eta_0 - \eta_\infty)}{[1 + (\tau\dot{\gamma})^m]} \quad (4)$$

$$\eta_a = \eta_\infty + \frac{(\eta_0 - \eta_\infty)}{[1 + (\lambda\dot{\gamma})^2]^N} \quad (5)$$

where $\dot{\gamma}$ is the shear rate (s^{-1}), η_a is the apparent viscosity (Pa s), η_0 is the zero-shear rate viscosity (Pa s), η_∞ is the infinite shear rate viscosity (Pa s), τ (s) and λ (s) are time constants, and m and N are dimensionless constants related to the power law exponent n by $m = 1 - n$ and $N = (1 - n)/2$ ($0 \leq N < 0.5$), for the case $\eta_\infty \ll \eta_a \ll \eta_0$. Since the high shear rate Newtonian viscosity was never approached in our study, the above equations were simplified (only three adjustable parameters), assuming $\eta_0 \gg \eta_\infty$.

As shown (Fig. 3, Tables 3 and 4) both models described the apparent viscosity shear rate data well, especially when there were experimental data in the plateau region, at low shear rates.

A comparison with experimental data demonstrates very good agreement with model predictions, as illustrated by magnitudes of RE (relative deviation error) (Tables 3 and 4). In general, the Cross model provided a slightly better fit. The Carreau model predicted zero shear rate viscosity values lower than the experimental ones; also, for this model, deviations between predicted and experimental values were observed at high shear rates (Fig. 3). As expected, due to the increase in shear-thinning behaviour with concentration, the values of η_0, m and N increased with

Table 3
Magnitudes of the Cross model parameters for steady simple shearing, obtained for crude tara gum (cTG), purified tara gum (pTG) and locust bean gum (LBG) samples

Samples	Concentration (wt%)	η_0 (Pa s)	τ (s)	m	RE[a]
cTG	1.29	57.9377	0.6989	0.8408	0.0173
	1.16	37.8104	0.5685	0.8405	0.0085
	1.03	18.6921	0.3993	0.7845	0.0140
	0.89	14.6262	0.3471	0.8059	0.0266
	0.78	7.7196	0.2353	0.7852	0.0129
	0.64	2.6478	0.1341	0.7305	0.0004
	0.50	0.8127	0.0568	0.6854	0.0124
	0.40	0.3514	0.0392	0.5939	0.0125
	0.25	0.0778	0.0131	0.4078	0.0049
pTG	1.19	65.2104	0.7360	0.8563	0.0111
	1.16	60.0526	0.7773	0.8422	0.0113
	1.02	35.7626	0.6590	0.8158	0.0126
	0.88	15.2637	0.3445	0.8175	0.0057
	0.78	8.6753	0.2648	0.7796	0.0093
	0.64	4.5960	0.1961	0.7619	0.0072
	0.50	1.5866	0.1123	0.7053	0.0161
	0.40	0.2735	0.0213	0.5934	0.0134
	0.25	0.1108	0.0127	0.4292	0.0146
LBG	1.00	4.3437	0.0632	0.7837	0.0041
	0.90	2.3938	0.0437	0.7660	0.0117
	0.80	1.8746	0.0367	0.7716	0.0087
	0.60	0.4902	0.0152	0.6671	0.0175
	0.40	0.1035	0.0025	0.5733	0.0144

[a] RE, relative deviation error $= \sum_{i=1}^{n} (|(x_{\exp,i} - x_{\mathrm{cal},i})/x_{\exp,i}|)/n$.

Table 4
Magnitudes of the Carreau model parameters for steady simple shearing, obtained for crude tara gum (cTG), purified tara gum (pTG) and locust bean gum (LBG) samples

Samples	Concentration (wt%)	η_0 (Pa s)	λ (s)	N	RE[a]
cTG	1.29	52.0983	1.2761	0.3665	0.0901
	1.16	32.6576	0.9628	0.3636	0.0727
	1.03	16.4715	0.8307	0.3208	0.0792
	0.89	13.3843	0.7913	0.3235	0.1021
	0.78	6.7015	0.4730	0.3204	0.0762
	0.64	2.1098	0.2327	0.3002	0.0685
	0.50	0.6370	0.1119	0.2634	0.0366
	0.40	0.2551	0.0809	0.2125	0.0192
	0.25	0.0495	0.0298	0.1281	0.0080
pTG	1.19	55.8862	1.1729	0.3812	0.0763
	1.16	50.8726	1.2006	0.3760	0.0765
	1.02	31.1623	1.1548	0.3563	0.0291
	0.88	13.0813	0.6037	0.3511	0.0687
	0.78	7.3825	0.4869	0.3241	0.0667
	0.64	3.6668	0.3208	0.3170	0.0551
	0.50	1.1911	0.1733	0.2885	0.0343
	0.40	0.2143	0.0624	0.1975	0.0274
	0.25	0.0793	0.0531	0.1236	0.0138
LBG	1.00	3.9870	0.1857	0.2797	0.0503
	0.90	2.2291	0.1204	0.2926	0.0499
	0.80	1.7076	0.1123	0.2686	0.0425
	0.60	0.4484	0.0528	0.2406	0.0433
	0.40	0.0952	0.0220	0.1518	0.0248

[a] RE, relative deviation error $= \sum_{i=1}^{n}(|(x_{\exp,i} - x_{\mathrm{cal},i})/x_{\exp,i}|)/n$.

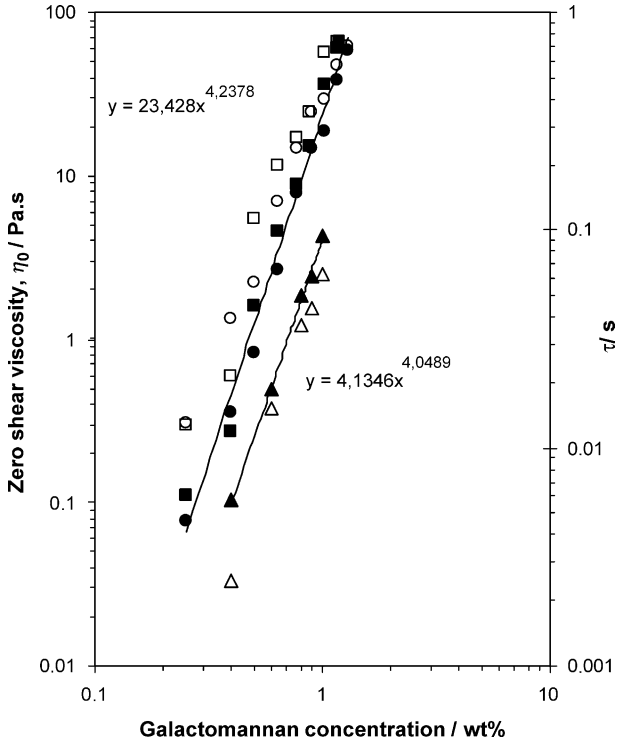

Fig. 4. Concentration dependence of zero shear viscosity, η_0 (full symbols) and time constant, τ (open symbols) for galactomannan samples: cTG (○), pTG (□) and LBG (△).

increasing concentration. Also, as said above, shear-thinning appears at lower shear rates when concentration increases; this means that the rate of formation of new entanglements diminishes as concentration increases; so, as can be seen in Tables 3 and 4, the time constants increase with concentration. The dependence of the Cross parameters η_0 and τ on galactomannan concentration is described by similar scaling laws for LBG and TG systems (Fig. 4).

The dependence of the specific viscosity at zero shear rate, η_{sp0}, on the coil overlap parameter, $C[\eta]$, is shown in Fig. 5. It is interesting to note that, by this reduction process, a similar behaviour for the two polymers is put in evidence. This was expected since both are galactomannans with similar chemical structures and conformations. If we assume, as described in literature for different polysaccharides (Castelain et al., 1987; Cuvelier & Launay, 1986), the existence of three different concentration regimes, dilute, semi-dilute and concentrated, it is possible, in principle, to define two critical concentrations, C^* and C^{**}, delimiting these regimes. From our data in Fig. 5, it is not possible to determine C^* (the incipient overlap concentration, the limit for the dilute regime) but we can make an estimation of C^{**} (the limit of the semi-dilute regime, the concentration beyond which a concentrated region is defined where the chain dimensions become independent of concentration); this would be about $7.76/[\eta]$ giving $C^{**} \sim 0.7$ wt% for LBG,

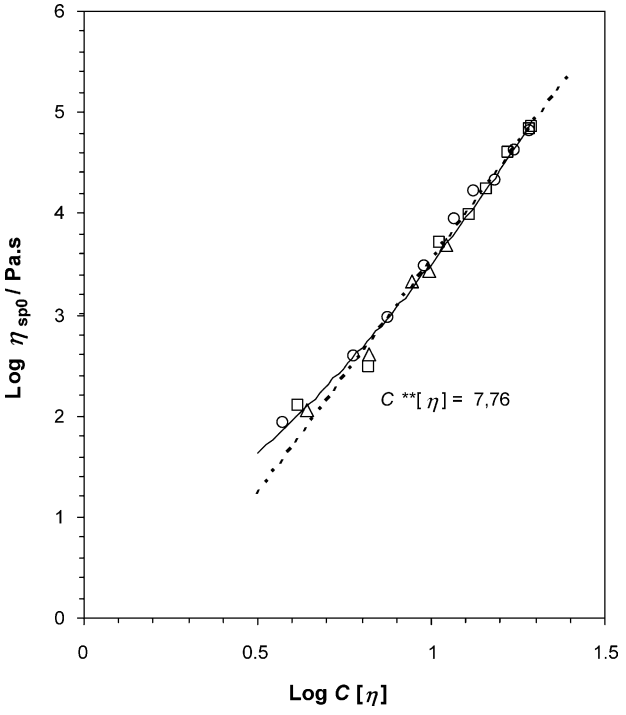

Fig. 5. Specific viscosity at zero shear rate (η_{sp0}) as a function of $C[\eta]$ in a log–log plot for galactomannans solutions: cTG (○), pTG (□) and LBG (△), measured at 25 °C.

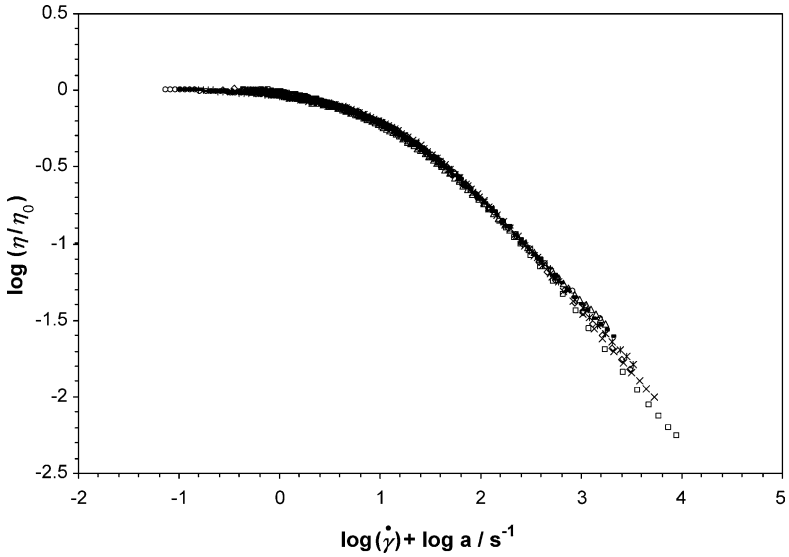

Fig. 6. Shear rate/concentration superposition for galactomannan solutions, at 25 °C. Master curve at the reference concentration of 1 wt% LBG. Symbols: 1.29% cTG (□), 0.89% cTG (○), 0.64% cTG (△), 0.88% pTG (×), 0.78% pTG (*), 0.64% pTG (¯), 1.0%LBG (−), 0.9%LBG (◇) and 0.8%LBG (+).

$C^{**} \sim 0.47$ wt% for pTG and $C^{**} \sim 0.52$ wt% for cTG. The concentrated domain ($C > C^{**}$) is characterized, as expected, by a power law dependence of viscosity on concentration. For typical polymers, the exponent is usually found to be in the range 3–4. In our case, a significantly higher value (4.7) was found; perhaps, this is related to a relatively high rigidity of LBG and TG backbones as compared to typical polymers. This value is in good agreement with previous results obtained for galactomannans (Andrade et al., 1999; da Silva et al., 1992). A value of ~3.4 obtained by Morris et al. (1981) for several random coil polysaccharides. However, they observed a greater concentration dependence of viscosity for guar gum and locust bean gum (~4). Their interpretation of this behaviour is that, for both galactomannans in this concentration range, normal polymer entanglement is augmented by chain–chain association, as in solid state.

Also, for this concentrated regime, it was possible to obtain a viscosity (flow) master curve, after performing a concentration-dependent shift using the 1 w% LBG solution as the reference (Fig. 6). It can be seen that this time–concentration superposition principle is valid for these galactomannans in this concentration range (within the accessible range of shear rates).

It was necessary to use both vertical and horizontal shifts to obtain the superposition of the different flow curves. The values of these shifts are presented in Fig. 7. Both the vertical shift, which is given by the ratio of the zero shear viscosities of the solution under consideration and the reference solution, and the horizontal shift (which represents the concentration shift factor) increase with concentration, for each galactomannan; this is consistent with the increasing degree of entanglement of the systems.

3.3. Rheological behaviour under dynamic shear

The frequency sweeps ('mechanical spectra') for both galactomannan solutions show the typical shape for macromolecular solutions (Fig. 8): at low frequencies (terminal zone), the dissipative modulus, G'', is higher than the conservative one (G') whereas, at higher frequencies, G' is predominant. Both curves tend asymptotically to

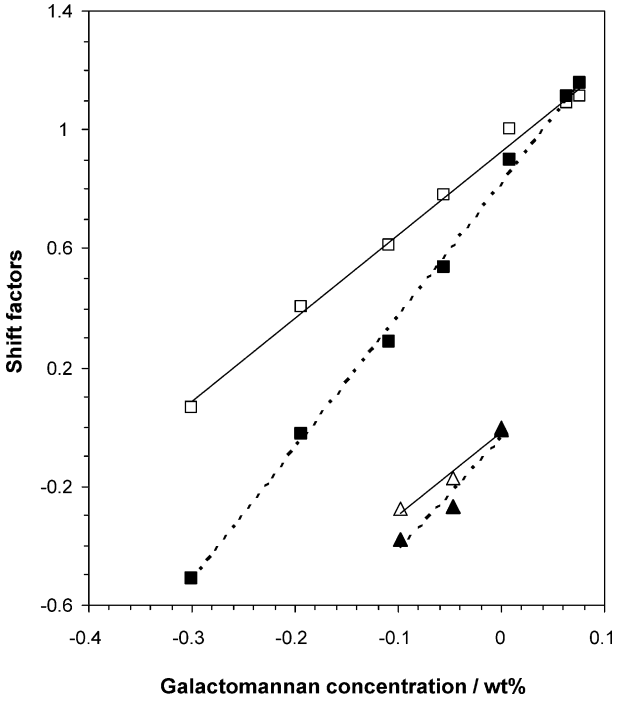

Fig. 7. Shift factors (horizontal: open symbols; vertical: full symbols) used for the concentration superposition of the flow data obtained for galactomannan solutions, at 25 °C: pTG (□) and LBG (△).

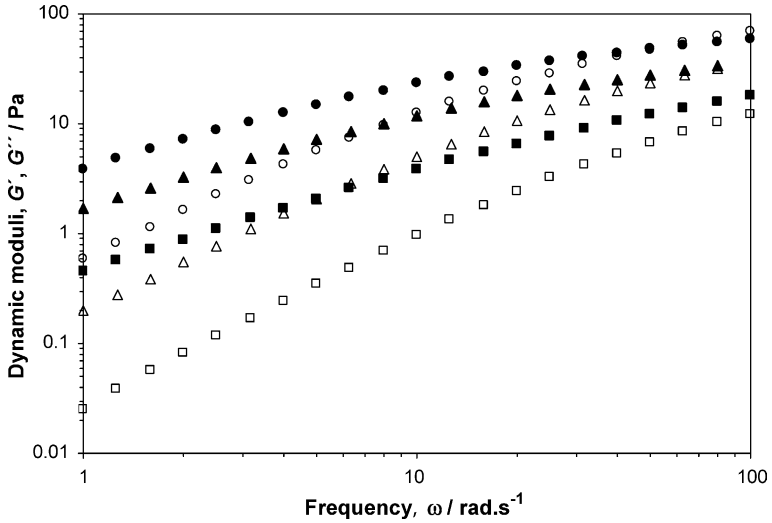

Fig. 8. Mechanical spectra of LBG solutions, at 25 °C (G': open symbols, G'': full symbols; 0.6% (□), 0.8% (△), 1% (○)).

the characteristic slopes of 1 and 2 for G'' and G', respectively. The first G'–G'' crossover, marking the low-frequency limit of the elastic plateau is visible for the higher concentrations in Fig. 8. This cross-over frequency decreases as concentration increases as a consequence of increasing relaxation times.

As we did for flow curves, it is possible to superpose all curves (of LBG and TG at different concentrations) by shifting along the two axes and obtain master curves for G' and G''. Fig. 9 shows the master curves obtained by this procedure with the 1 wt% LBG solution as reference. The vertical and horizontal shift factors were the same for both G′ and G″ curves. Horizontal shifts were equal to those in Fig. 7 for flow while vertical shifts decrease with concentration for each galactomannan (not shown). From the master curves in Fig. 9, we can see that the characteristic slopes would be only approached at frequencies <0.3 rad s^{-1}, in the case of the 1 wt% LBG solution.

3.4. Modelling the rheological behaviour under dynamic shear

Two mechanical models were used to fit the experimental viscoelastic data: the generalized Maxwell model with four elements (Eqs. (6) and (7)) and the Friedrich–Braun model (Eqs. (8) and (9)) (Friedrich & Braun, 1992). Both models have been already successfully used by other authors for describing the rheological behaviour of guar gum galactomannan (Oblonsek et al., 2003), and other polysaccharide systems (Manca et al., 2001; Zupancic & Zumer 2001).

In the generalized Maxwell model, the values of the overall G' and G'', at any frequency, are given by the sum of

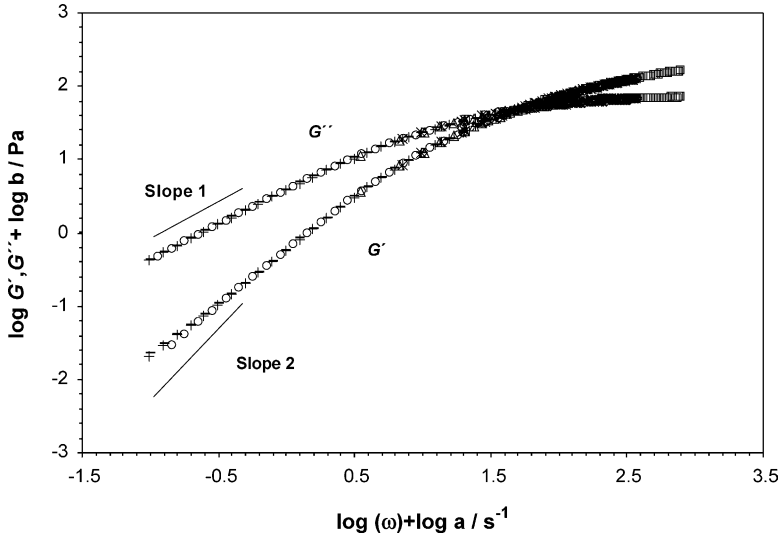

Fig. 9. Frequency/concentration superposition of the dynamic moduli (G' and G'') of galactomannan solutions for a concentration reference of 1 wt% LBG, measured at 25 °C. Symbols: 1.29% cTG (□), 0.89% cTG (○), 0.64% cTG (△), 0.88% pTG (×), 0.78% pTG (*), 0.64% pTG (¯), 1.0%LBG (−), 0.9%LBG (◇) and 0.8%LBG (+).

four contributions from four Maxwell elements in parallel

$$G'(\omega)=\frac{G_1(\omega\theta_1)^2}{1+(\omega\theta_1)^2}+\frac{G_2(\omega\theta_2)^2}{1+(\omega\theta_2)^2}+\frac{G_3(\omega\theta_3)^2}{1+(\omega\theta_3)^2}+\frac{G_4(\omega\theta_4)^2}{1+(\omega\theta_4)^2} \quad (6)$$

$$G''(\omega)=\frac{G_1\omega\theta_1}{1+(\omega\theta_1)^2}+\frac{G_2\omega\theta_2}{1+(\omega\theta_2)^2}+\frac{G_3\omega\theta_3}{1+(\omega\theta_3)^2}+\frac{G_4\omega\theta_4}{1+(\omega\theta_4)^2} \quad (7)$$

where G_i is the elastic modulus, ω is the angular frequency and θ_i is the terminal relaxation time. The dynamic response of a viscoelastic liquid over a range of frequencies can be modelled by choosing a range of Maxwell elements with appropriate values of G and θ chosen to cover the range used in the experiment for which G' and G'' values are available.

Alternatively, the Friedrich and Braun model, which is based on fractional derivatives, can be used to achieve a satisfactory data correlation. In oscillatory shear conditions, G' and G'' can be expressed as:

$$G'(\omega)=G_e+\Delta G\frac{(\lambda_F\omega)^d\left[\cos\left(\frac{\pi}{2}d\right)+(\lambda_F\omega)^c\cos\left(\frac{\pi}{2}(d-c)\right)\right]}{1+2(\lambda_F\omega)^c\cos\left(\frac{\pi}{2}c\right)+(\lambda_F\omega)^{2c}} \quad (8)$$

$$G''(\omega)=\Delta G\frac{(\lambda_F\omega)^d\left[\sin\left(\frac{\pi}{2}d\right)+(\lambda_F\omega)^c\sin\left(\frac{\pi}{2}(d-c)\right)\right]}{1+2(\lambda_F\omega)^c\cos\left(\frac{\pi}{2}c\right)+(\lambda_F\omega)^{2c}} \quad (9)$$

where G_e is the equilibrium modulus when the frequency tends to zero, ΔG is a parameter that rules the magnitude of the viscoelastic response, λ_F is a characteristic time and the exponents c and d are derivation orders of the differential operators. The model describes liquid-like response if $G_e=0$. When $c=d=1$ and $G_e=0$, this model coincides with the Maxwell model and, then, λ_F becomes the relaxation time of the fluid.

In Fig. 10, the results of the fitting of the two models to experimental data for LBG are shown. The full and dotted lines represent the best fits to both models. Similar high fitting quality of the dynamic moduli was found in the case of tara gum samples (not shown).

As a result of this fitting, relaxation spectra of each galactomannan sample can be evaluated (Fig. 11). At low concentrations, the elastic modulus, G_i, continuously decreases with increasing relaxation time λ_i. The increase of galactomannan concentrations leads to a gradual shifting of the relaxation spectrum to higher values. For cTG and LBG systems, typical profiles for polysaccharide solutions were obtained, with increasing contribution of higher relaxation times for increasing polymer concentration. For purified tara gum, (Fig. 11(b)) the profiles of relaxation spectra show a somewhat different shape; also, higher values of G_i than for other galactomannan samples were obtained.

In the Friedrich–Braun model, G_e was set equal to zero, thereby reducing the number of adjustable parameters. These were determined by applying the fitting procedure simultaneously to $G'(\omega)$ and $G''(\omega)$.

The parameters of the Friedrich and Braun model are presented in Fig. 12. The variation of model parameters exhibit similar trends for the three galactomannan samples: ΔG and λ_F gradually increase with increasing concentration whereas a gradual decrease is observed in the derivation order d.

The Cox–Merz rule was applied to correlate dynamic and steady shear properties. The magnitude of the apparent viscosity in steady shear and the magnitude of the complex viscosity in oscillatory shear were compared at equal values

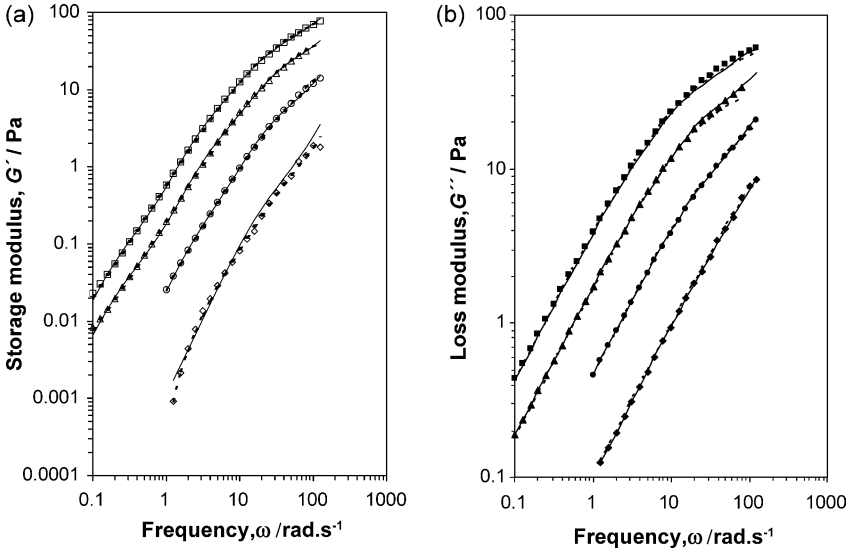

Fig. 10. Storage modulus G' (a) and loss modulus G'' (b) vs oscillation frequency for LBG at different concentrations and 25 °C: 0.4% (◇), 0.6% (○), 0.8% (△) and 1.0% (□). Continuous lines represent predictions of the Generalized Maxwell model and dotted lines those of the Friedrich–Braun model.

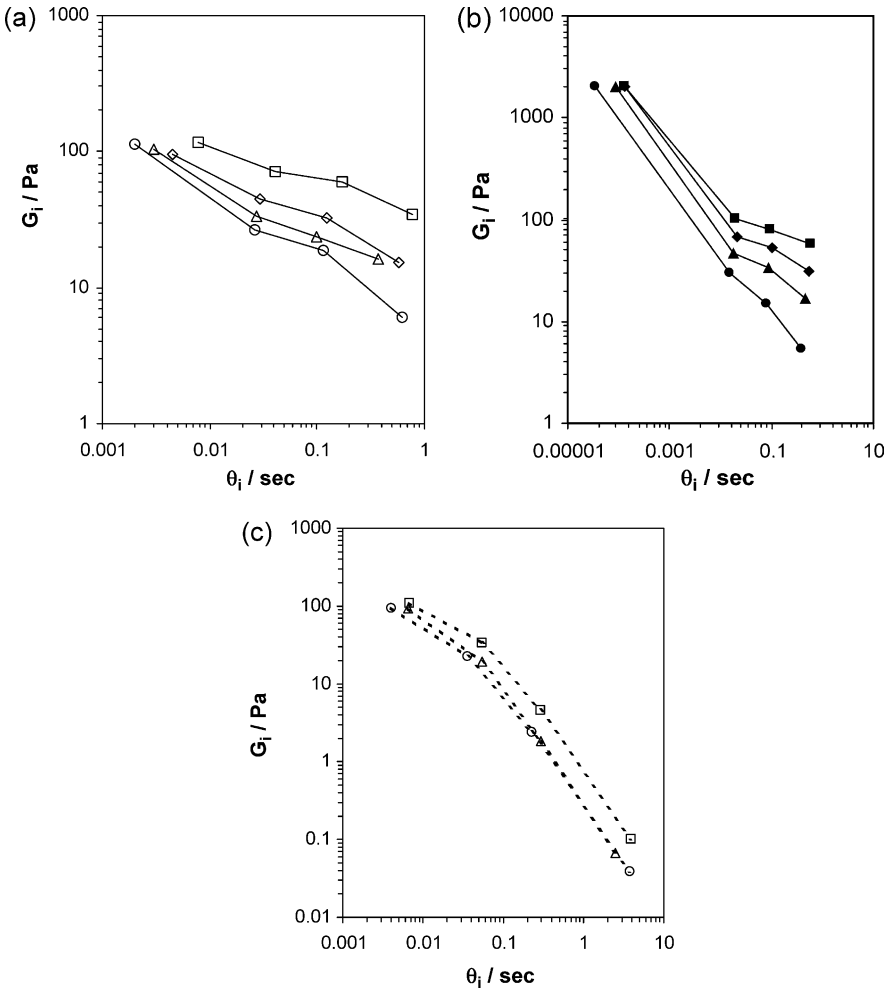

Fig. 11. The relaxation spectra of crude tara gum systems (a), purified tara gum systems (b) and locust bean gum systems (c) at different galactomannan concentrations. Symbols: 0.78% cTG (–○–), 0.89% cTG (—△—), 1.03% cTG (—◇—), 1.29% cTG (—□—), 0.64% pTG (—●—), 0.88% pTG (—▲—), 1.02% pTG (—◆—), 1.19% pTG (—■—), 0.8% LBG (··○··), 0.9% LBG (···△···) and 1.0% LBG (··□··).

of shear rate and frequency. In Fig. 13, the results obtained for LBG solutions are presented; these solutions followed satisfactorily the correlation of Cox–Merz with $|\eta^*|(\omega)$ and $\eta(\dot{\gamma})$ almost superimposed. A similar behaviour was observed for TG solutions (not shown). We could conclude that both galactomannans behave like ordinary polysaccharides. Similar results were obtained by Andrade et al. (1999), da Silva et al. (1993) and Ross-Murphy (1995) with several galactomannan dispersions.

A common feature observed in these results was that the dynamic viscosity (η') approached the zero shear rate viscosity at low frequency and shear rate. With increasing frequency and shear rate, apparent viscosity in steady shear and dynamic viscosity began to diverge gradually, with the expected more rapid decrease of dynamic viscosity with frequency than apparent viscosity with shear rate; this can be attributed to the very different molecular motions involved in the dynamic and steady shears at high frequency and shear rate (Ferry, 1980). With increasing concentration of galactomannan, the dynamic viscosity becomes more divergent as shown in Fig. 13.

4. Conclusions

The results obtained showed that both galactomannans exhibited quite similar rheological properties, in the range of concentrations and shear rates/frequencies studied. The dependence of the specific viscosity at zero shear rate, η_{sp0}, on the coil overlap parameter, $C[\eta]$, put in evidence a similar behaviour for the two polysaccharides; results supported the random coil-type behaviour for both galactomannans. The dependence of the Cross parameters η_0 and τ on galactomannan concentration is described by similar scaling laws for LBG and TG systems. Also, time–concentration superposition holds for their solutions, allowing master curves to be found for both the viscous and linear viscoelastic response in shear flow. The similar

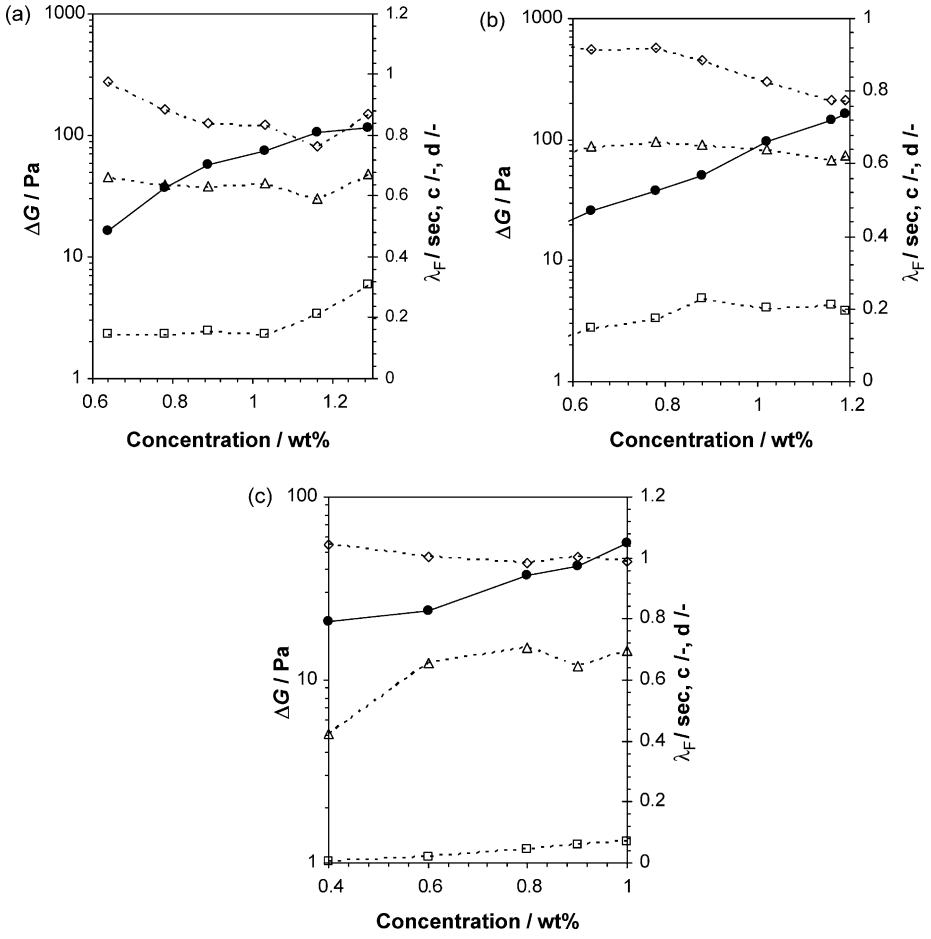

Fig. 12. Parameters of Friedrich and Braun models (Eqs. (8) and (9)) for crude tara gum systems (a), purified tara gum systems (b), and locust bean gum systems (c): ΔG (○), λ_F (□), c (△) and d (◇).

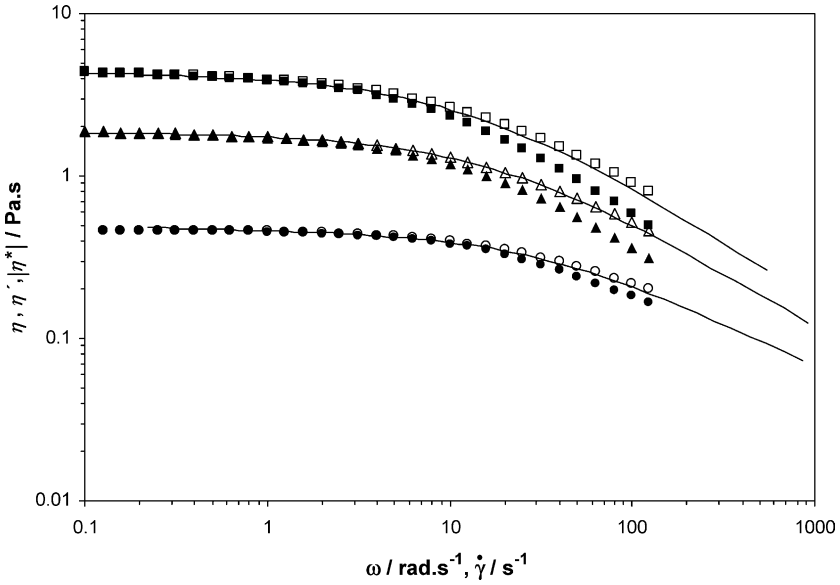

Fig. 13. Cox–Merz plot for LBG solutions at different concentrations, at 25 °C. 0.6% (○), 0.8% (△), 1.0% (□); η (continuous line), η' (full symbols), $|\eta^*|$ (open symbols).

profile observed probably reflects the existence of non-specific physical entanglements in TG and LBG solutions.

Acknowledgements

This work was financially supported by Fundação para a Ciência e a Tecnologia (project POCTI/2000/QUI/36452). The author W. Sittikijyothin is indebted to Fundação para a Ciência e a Tecnologia for the PhD grant No. SFRH/BD/6041/2001.

References

Alais, C., & Linden, G. (1991). *Food biochemistry*. New York: Ellis Horwood.

Alves, M. M., Antonov, Y. A., & Gonçalves, M. P. (1999). On the incompatibility of alkaline gelatin and locust bean gum in aqueous solution. *Food Hydrocolloids*, *13*, 77–80.

Alves, M. M., Garnier, C., Lefebvre, J., & Gonçalves, M. P. (2001). Microstructure and flow behaviour of liquid water–gelatin–locust bean gum systems. *Food Hydrocolloids*, *15*, 117–125.

Andrade, C. T., Azero, E. G., Luciano, L., & Gonçalves, M. P. (1999). Solution properties of the galactomannans extracted from the seeds of *Caesalpinia pulcherrima* and *Cassia javanica*: comparison with locust bean gum. *International Journal of Biological Macromolecules*, *26*, 181–185.

Batlle, I., & Tous, J. (1997). *Carob tree Ceratonia siliqua* L.: Promoting the conservation and use of underutilized and neglected crops 17. Rome: Institute of Plant Genetics and Crop Plant Research.

Carreau, P. J. (1972). Rheological equations from molecular network theories. *Transactions of the Society of Rheology*, *16*, 99–127.

Castelain, C., Doublier, J. L., & Lefebvre, J. (1987). A study of the viscosity of cellulose derivatives in aqueous solutions. *Carbohydrate Polymers*, *7*, 1–16.

Coimbra, M. A., Delgadillo, I., Waldron, K. W., & Selvendran, R. R. (1996). Isolation and analysis of cell wall polymers from olive pulp. In H. F. Linskens, & J. F. Jackson, *Modern methods of plant analysis. Plant cell wall analysis* (Vol. 17) (p. 19). Berlin: Springer.

Courtois, J. E., & Le Dizet, P. (1966). Action de l'a-galactoside du café sur quelques galactomannanes. *Carbohydrate Research*, *3*, 55–192.

Cross, M. M. (1965). Rheology of non Newtonian fluids: a new flow equation for pseudoplastic systems. *Journal of Colloid Science*, *20*, 417–437.

Cuvelier, G., & Launay, B. (1986). Concentration regimes in xanthan gum solutions deduced from flow and viscoelastic properties. *Carbohydrate Polymers*, *6*, 321–333.

da Silva, J. A. L., & Gonçalves, M. P. (1990). Studies on a purification method for locust bean gum by precipitation with isopropanol. *Food Hydrocolloids*, *4*, 277–287.

da Silva, J. A. L., Gonçalves, M. P., & Rao, M. A. (1992). Rheological properties of high-methoxyl pectin and locust bean gum solutions in steady shear. *Journal of Food Science*, *57*, 443–448.

da Silva, J. A. L., Gonçalves, M. P., & Rao, M. A. (1993). Viscoelastic behaviour of mixtures of locust bean gum and pectin dispersion. *Journal of Food Engineering*, *18*, 211–228.

da Silva, J. A. L., & Rao, M. A. (1992). Viscoelastic properties of food hydrocolloid dispersions. In M. A. Rao, & J. F. Steffe (Eds.), *Viscoelastic properties of foods* (pp. 285–315). London: Elsevier.

Dea, I. C. M., Clark, A. H., & Mc Cleary, B. V. (1986). Effect of galactose substitution patterns on the interaction properties of galactomannans. *Carbohydrate Research*, *147*, 275–294.

Dea, I. C. M., Morris, E. R., Rees, D. A., Welsh, E. J., Barnes, H. A., & Price, J. (1977). Associations of like and unlike polysaccharides: mechanism and specificity in galactomannans, interacting bacterial polysaccharides and related systems. *Carbohydrate Research*, *57*, 249–272.

Doublier, J. L., & Launay, B. (1981). Rheology of galactomannan solutions: comparative study of guar gum and locust bean gum. *Journal of Texture Studies*, *12*, 151–172.

Fernandes, P. B., Gonçalves, M. P., & Doublier, J. L. (1991). A rheological characterization of kappa-carrageenan/galactomannan mixed gels: a comparison of locust bean gum samples. *Carbohydrate Polymers*, *16*, 253–274.

Ferry, J. D. (1980). *Viscoelastic properties of polymers*. New York: Wiley.

Food and Nutrition Board-National Research Council (1981). *Food chemicals codex*. Washington, DC: National Academy Press.

Friedrich, C., & Braun, H. (1992). Generalized Cole–Cole behaviour and its rheological relevance. *Rheologica Acta*, *31*, 309–322.

Gaisford, S. E., Harding, S. E., Mitchell, J. R., & Bradley, T. D. (1986). A comparison between the hot and cold water soluble fractions of two locust bean gum samples. *Carbohydrate Polymers*, *6*, 423–442.

Gonçalves, M.P. (1984). Coprecipitation des proteins du plasma bovin avec des polyosides anioniques. *Etude rheologique des coprecipites et des interactions entre la serumalbumine bovine et le lambda-carraghénane ou l'alginate de sodium*. Doctor Engineer Thesis. University of Clermont Ferrand II, CNRS No DI 128, France.

Manca, S., Lapasin, R., Partal, P., & Gallegos, C. (2001). Influence of surfactant addition on the rheological properties of aqueous welan matrices. *Rheologica Acta*, *40*, 128–134.

Mc Cleary, B. V., Clark, A. H., Dea, I. M. C., & Rees, D. A. (1985). The fine structure of carob and guar galactomannans. *Carbohydrate Research*, *139*, 237–260.

Mc Cleary, B. V., & Neukom, H. (1982). Effect of enzymatic modification on the solution and interaction properties of galactomannans. *Progress Food and Nutrition Science*, *6*, 109–118.

Morris, E. R. (1990). Mixed polymer gels. In P. Harris (Ed.), *Food gels* (pp. 291–359). London: Elsevier.

Morris, E. R., Cutler, A. N., Ross-Murphy, S. B., Rees, D. A., & Price, J. (1981). Concentration and shear rate dependence of viscosity in random coil polysaccharide solutions. *Carbohydrate Polymers*, *1*, 5–21.

Oblonsek, M., Sostar-Turk, S., & Lapasin, R. (2003). Rheological studies of concentrated guar gum. *Rheologica Acta*, *42*, 491–499.

Robinson, G., Ross-Murphy, S. B., & Morris, E. R. (1982). Viscosity–molecular weight relationships, intrinsic chain flexibility, and dynamic solution properties of guar galactomannan. *Carbohydrate Research*, *107*, 17–32.

Ross-Murphy, S. B. (1995). Structure–property relationships in food biopolymer gels and solutions. *Journal of Rheology*, *39*, 1451–1463.

Ruiz-Ángel, M. J., Simó-Alfonso, E. F., Mongay-Fernández, C., & Ramis-Ramos, G. (2002). Identification of leguminosae gums and evaluation of carob–guar mixtures by capillary zone electrophoresis of protein extracts. *Electrophoresis*, *23*, 1709–1715.

Zupancic, A., & Zumer, M. (2001). Viscoelastic properties of hydrophilic polymers in aqueous dispersions. *Acta Chimica Slovenica*, *48*, 469–486.